ISSN 1068-1620, Russian Journal of Bioorganic Chemistry, 2020, Vol. 46, No. 7, pp. 1295–1303. © Pleiades Publishing, Ltd., 2020.
Russian Text © The Author(s), 2019, published in Khimiya Rastitel'nogo Syr'ya, 2019, No. 1, pp. 39–50.

PLANT BIOPOLYMERS

Dispersibility of Nanocrystalline Cellulose in Organic Solvents

M. I. Voronova[a, 1], O. V. Surov[a], N. V. Rubleva[a], N. E. Kochkina[a], and A. G. Zakharov[a]

[a] *Krestov Institute of Solution Chemistry, Russian Academy of Sciences, Ivanovo, 153045 Russia*

Received June 27, 2018; revised September 18, 2018; accepted September 21, 2018

Abstract—Aqueous suspensions of nanocrystalline cellulose (NCC) were obtained by sulfuric acid hydrolysis using the standard procedure. Suspensions, films, and aerogel of NCC were characterized by various methods: the degree of polymerization was determined, elemental analysis was carried out, the degree of crystallinity and crystallite size were calculated on the basis of X-ray data, and the morphology of NCC aerogels was studied using scanning electron microscopy. The particle size of the NCC was determined using a transmission electron microscope, a scanning atomic force microscope, and the method of dynamic light scattering. NCC hydrosols with different pH were used to prepare lyophilized NCC samples. From NCC hydrosols with pH 2.2, by gradual replacement of water with an organic solvent, NCC organogels with acetone, acetonitrile, and ethanol were obtained. The dispersion of lyophilized NCC and NCC organogels (acetone, acetonitrile, and ethanol) in water and in 11 organic solvents was investigated. The effect of the pH of the initial aqueous suspension of the NCC and the solvent forming the NCC organogel on the repeated dispersibility of the NCC is shown. The optimum pH value of the initial aqueous suspension of NCC was determined, which determines the maximum dispersibility of the lyophilized samples in each specific solvent. Acetone, acetonitrile, and ethanol organogels are dispersed in most of the solvents studied with the formation of particles less than 100 nm in diameter.

Keywords: nanocrystalline cellulose, re-dispersibility, particle size

DOI: 10.1134/S106816202007016X

INTRODUCTION

Nanocrystalline cellulose (NCC) is a product of controlled hydrolysis of cellulose-containing material. The sizes of the obtained NCC particles [1], depending on the source of cellulose and the conditions of hydrolysis, usually vary from several dozen to several hundred nanometers in length and from about 3 to 50 nm in diameter. The aspect ratio (the ratio of length to the smallest transverse dimension) is 10–30 for NCC obtained from cotton cellulose, and about 70 for NCC obtained from animal cellulose (tunicin).

The properties of nanocrystalline cellulose—anisotropic shape of particles, high mechanical strength [2], the possibility of chemical modification of surface hydroxyl groups [3], and the formation of a chiral nematic liquid-crystalline phase in aqueous suspensions and films [4]—attract much attention to NCC from the point of view of development of new functional materials. The use of NCC in the composition of a composite can improve its mechanical, optical, and sorption properties or impart the composite with new properties, for example, biodegradation [5, 6].

Sulfuric [7] and hydrochloric [8] acids are most often used to obtain NCC; nitric [9], hydrobromic, or phosphoric acid [10, 11] are used less often.

In recent years, organic carboxylic acids [12–15], as well as mixtures of various acids [16, 17], have been increasingly used to obtain NCCs.

Other methods for NCC preparation include enzymatic hydrolysis [18, 19], hydrolysis in the presence of heteropolyacids (for example, tungstophosphoric acid) [20, 21], salts of multivalent metals [22, 23], treatment with ionic liquids [24–26], oxidation of cellulose [27–30], and a number of others [31] and are used, as a rule, in combination with other chemical, mechanical, or ultrasonic treatment methods.

At present, the standard procedure for the preparation of NCC includes hydrolysis with 62–65% sulfuric acid at 45–50°C, washing using repeated centrifugation cycles, dialysis, ion exchange treatment, and sonication. When sulfuric acid is used, hydrolysis results in the surface hydroxyl groups replaced by sulfo groups, while the negative charge of the surface stabilizes the aqueous dispersions of NCC particles due to electrostatic repulsion [32].

When working with NCC, the problem of redispersion of dried aqueous suspensions arises due to irreversible aggregation of particles and loss of functional properties inherent to NCC nanoparticles. Redispersibility is important to restore the unique properties of NCC suspensions after product drying for storage or transportation. Commercialization and industrial use

[1] Corresponding author: e-mail: miv@isc-ras.ru.

requires NCC to be supplied dry and redispersed at the point of use to minimize product size and weight and hence shipping costs. Drying prevents the growth of bacteria and microorganisms in the NCC and is often a necessary stage of solvent replacement before dispersing the NCC in organic solvents or polymers to obtain nanocomposites.

The preparation of polymer composites requires mixing the NCC sol with a polymer solution in the same solvent. Therefore, to create composites with polymers insoluble in water, it is necessary to obtain NCC sols in organic solvents.

The easiest way to obtain such sols is by direct dispersion of dried NCC in an organic solvent. Drying of aqueous suspensions of NCC by natural evaporation of water leads to irreversible aggregation of NCC particles and the impossibility of their redispersion. Therefore, for repeated dispersion, freeze drying of NCC is used [33, 34].

Another way to obtain organic sols is to gradually replace the solvent (water with an organic solvent). Replacing water with an organic solvent [35] can be carried out using several cycles of centrifugation. If it is necessary to obtain an NCC sol in a solvent immiscible with water, an intermediate solvent is used [36]. For water-miscible solvents, the boiling point of which is higher than the boiling point of water, the method [37] of replacing the solvent is used, based on the evaporation of water under vacuum.

Despite the urgency of the existing problem, a small number of works have been devoted to the issues of redispersion of NCC in polar and nonpolar organic solvents without the use of surfactants and modification of the surface of NCC particles.

In [35], the dispersion of NCC particles, the surface of which does not have charged functional groups, was studied (NCC was obtained by hydrolysis with HCl). Out of 21 investigated solvents, stable suspensions were obtained in 12. Studies have shown that NCC tends to disperse in solvents with high dielectric constant, as well as high values of donor and acceptor numbers.

On the contrary, in [38], comparing the dispersion in water and organic solvents of lyophilized NCC obtained by hydrolysis in the presence of H_2SO_4 or HCl, the authors conclude that the presence of surface sulfate groups is a necessary condition for dispersing NCC in polar aprotic solvents. In proton–donor solvents, NCC is dispersed regardless of the presence of a charge.

In [33], the role of small amounts of water in the formation of stable suspensions of NCC in two polar solvents, DMSO and DMF, was shown. NCC was obtained by hydrolysis with H_2SO_4 and freeze-dried.

In [39], the dispersion of NCC in formamide and its derivatives, *N*-methylformamide and *N*,*N*-dimethylformamide, was studied using a solvent replacement method based on the evaporation of water under reduced pressure. The authors conclude that the main parameter of the solvent, which affects the dispersibility, is the dielectric constant of the solvent.

In a number of works [33, 39] it is noted that the lyophilized neutralized form of NCC is easily dispersed in polar organic solvents (dimethyl sulfoxide, dimethylformamide, formamide).

The purpose of this article is to investigate the effect of the pH of NCC hydrosols subjected to freeze-drying on the ability to redisperse in water and polar organic solvents, as well as to investigate the process of dispersion of NCC organogels obtained in three different solvents (acetonitrile, acetone, ethanol). The criterion for redispersibility was conventionally considered the size of the NCC particles and the colloidal stability of the suspensions during the day. The size of the NCC particles was determined by the method of dynamic light scattering, the colloidal stability of the suspensions was assessed visually by the precipitation and clarification of the suspension.

EXPERIMENTAL

Materials. To obtain NCC, commercial microcrystalline cellulose (MCC) (Cellulose, powder ~20 micron, Sigma-Aldrich), bidistilled water, and sulfuric acid (chemically pure grade, GOST 4204-77, Khimmed) were used.

The following solvents were used in the work: dimethyl sulfoxide (DMSO), dimethylformamide (DMF), ethylene glycol, chloroform (Sigma-Aldrich), dioxane-1,4 (Macron Fine Chemicals™), acetonitrile, methanol, ethanol, isopropanol, acetone, and toluene (Khimmed). All solvents were chemically pure or extra pure and were used without additional purification.

Methods. The general experimental technique, including the preparation of aqueous suspensions of NCC, the aerogel, and NCC organogels, is schematically presented in the electronic supplementary materials.

Preparation of the aqueous suspension of NCC. NCC hydrosols were obtained by sulfuric acid hydrolysis of MCC by the method described earlier [7]. Hydrolysis of MCC (suspension concentration 0.025 g/mL) was carried out in a sulfuric acid solution (62%) at 50°C for 2 h under vigorous stirring. After hydrolysis, the suspension was washed with water, followed by centrifugation (10 min at 8000 rpm). The centrifugation stage was terminated after 5–6 washes. Then the NCC suspension was sonicated (Sonorex DT100 Bandelin) for 15–30 min. The NCC aqueous suspension was purified using the TOKEM MV-50 (R) ion-exchange resin for 3 days. The NCC yield was 30–35%.

The cellulose obtained in this way is an acidic form of NCC (pH of an aqueous suspension is 2.2). Neutralization of the acidic form of NCC with 0.1 M

NaOH solution to pH 4.0; 6.6; and 9.5 yielded neutralized forms of NCC.

Freeze-drying of NCC, preparation of the aerogel. The NCC hydrosol with a concentration of 10–14 g/L was lyophilized. Samples were prefrozen at –40°C for 2 days, then placed in a freeze dryer. The drying process took place at a pressure of 6 Pa, a temperature of –54°C for 48 h. The samples obtained are designated as NCC-2.2, NCC-4.0, NCC-6.6, NCC-9.5, which corresponds to the pH of the NCC hydrosol subjected to freeze-drying.

Preparation of NCC organogels. NCC organogels were obtained from NCC hydrosols by gradual replacement of water with an organic solvent miscible with water. Acetone, acetonitrile, or ethanol were used as solvents for the preparation of organogels. The organic solvent was carefully added to the surface of the aqueous NCC suspension to prevent mixing and to ensure the formation of an organic layer over the aqueous suspension. The organic layer was replaced 1–2 times a day until the NCC at the bottom collected into a homogeneous gel (usually 5–7 days). During the process, the organic layer was slightly shaken to facilitate solvent exchange. The content of NCC in organogels was determined gravimetrically. The gels were weighed wet and dry. The NCC content in the acetonitrile gel was 8%; in acetone, 6%, and in ethanol, 5%.

Redispersing. Lyophilized NCC and organogels were redispersed in distilled water and organic solvents for 2 h with stirring and sonicated for 30 min (Sonorex DT100 Bandelin).

Research methods. The size of the NCC particles was determined using an EMV-100L transmission electron microscope (TEM) (Russia), a Solver P47-PRO scanning atomic force microscope (AFM) (Russia), and dynamic light scattering (DLS) using a Zetasizer Nano ZS (Malvern Instruments Ltd, UK) particle size analyzer.

Images of NCC particles were obtained using TEM at an accelerating voltage of 50 kV. Before photographing, a drop of a dilute aqueous suspension of NCC (1 g/L) was treated with ultrasound, applied to a carbon-coated microscope grid, and dried.

Images of the surface of the NCC film were obtained using AFM in a semicontact scanning mode.

The particle size distribution in aqueous and organic NCC sols was determined by dynamic light scattering (radiation wavelength 633 nm) on a Zetasizer Nano ZS instrument (Malvern Instruments Ltd, UK) operating in the range of 0.3 nm–6 μm. The measurements were carried out at a sol concentration of 0.1 mg/mL in disposable polystyrene cuvettes. During measurements, the cuvette temperature was set to 20°C. The obtained particle size values are the results of averaging over five successive measurement cycles. The value obtained in each cycle is, in turn, the result of automatic processing of 10–15 measurements.

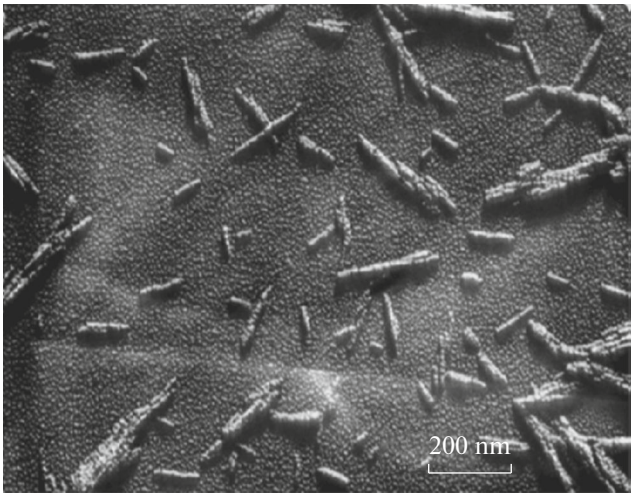

Fig. 1. Micrograph of NCC particles obtained using the EMV-100L TEM. Scale bar 200 nm.

The surface charge of NCC particles in an aqueous suspension was estimated by the value of the ζ-potential (Zetasizer Nano ZS). The values of the ζ-potential are the results of averaging over five successive measurement cycles.

The concentration of surface sulfo groups of NCC was assessed by elemental analysis for sulfur content (analyzer Flash EA-1112, Thermo Quest, Italy).

The degree of cellulose polymerization was determined from the viscosity of its solution in cadoxen.

X-ray structural analysis of the films was carried out on a Bruker D8 Advance diffractometer (Germany) according to the Bragg–Brentano scheme using CuK_α radiation (λ = 0.1542 nm). The angular scanning range was 2°–35° with a step of 0.01°. A Vantec-1 high-speed counter was used. The pulse acquisition time at each scan point was 0.5 s. The Segal crystallinity index [40] was determined as

$$IC = \frac{I_{200} - I_a}{I_{200}},$$

where I_{200} is the intensity of the reflection 200 and I_a is the intensity of the amorphous halo (the minimum between peaks 200 and 110).

The crystallite sizes were calculated using the Scherrer formula [41]

$$L = \frac{0.9\lambda}{\beta\cos\theta},$$

where λ is the X-ray radiation wavelength, nm, β is the width of the analyzed reflection, rad, θ is the angular position of the reflection, deg. For the calculation, we used a reflection at $2\theta = 22.9°$.

Table 1. Characteristics of NCC

Parameters		Characteristics
[a]Particle size, nm	Length	200–400
	Diameter	10–20
[b]Hydrodynamic diameter, nm	Fraction 1	310 ± 20
	Fraction 2	60 ± 20
[b]Value of ζ-potential, mV		–40
[c]Sulfur content, %		0.65
[d]Polymerization degree		80
[e]Crystallinity index, %		83.8
[e]Crystallite surface size (200), nm		4.1

[a]Transmission electron microscopy (EMV-100L); scanning atomic force microscopy (Solver P47-PRO); [b]values for aqueous suspensions; dynamic light scattering (Zetasizer Nano-ZS); [c]elemental analysis (Flash EA-1112); [d]determined by the viscosity of NCC solutions in cadoxen; [e]X-ray diffraction analysis (Bruker D8 Advance).

Films of NCC samples for X-ray structural analysis and AFM imaging were obtained by natural evaporation of water at room temperature from aqueous suspensions with a concentration of 10 g/L.

To study the morphology of dried NCC samples, we used a LIRA3 TESCAN (Czech Republic) scanning electron microscope. The samples were recorded at an accelerating voltage of 5 kV in a high vacuum mode.

RESULTS AND DISCUSSION

Table 1 shows the main characteristics of the NCC obtained by sulfuric acid hydrolysis.

The TEM images show that the NCC particles have an anisotropic rod-like shape and are fairly uniformly distributed, although aggregates formed due to lateral interaction of particles are observed (Fig. 1). The AFM images of the NCC film surface also show individual rod-like NCC particles (Fig. 2b), as well as particle aggregates (Fig. 2a). The length of the particles varies approximately from 200 to 400 nm, the diameter of the NCC particles is approximately 10–20 nm (Table 1, Figs. 1, 2).

Experimental data on DLS in an aqueous suspension show a polydisperse character of the NCC particle size distribution. Two groups of particles can be distinguished with sizes of about 300 and 60 nm, respectively (Table 1, Fig. 1S of Supplementary Materials).

Aqueous suspensions of NCC exhibit high colloidal stability for a long time, which is due to the significant charge of sulfate groups grafted onto the surface of NCC particles in the course of sulfuric acid hydrolysis. According to the measurement results, the value of the ζ-potential of the NCC aqueous suspensions is –40 mV, the sulfur content (in the composition of surface sulfo groups) is 0.65% (Table 1).

Diffraction patterns of NCC films are shown in Fig. 3. Despite the low intensity of reflections, a diffraction peak at the Bragg angle $2\theta = 22.9°$ corresponding to the crystallographic plane (200) of cellulose I_β is clearly visible, as well as an implicitly expressed double peak in the region of $2\theta = 15°–17°$, which corresponds to planes (1–10) and (110) of cellulose I_β [42]. NCC films are characterized by a high crystallinity index (about 84%) and a crystallite size of about 4 nm (in the crystallographic plane (200)) (Table 1).

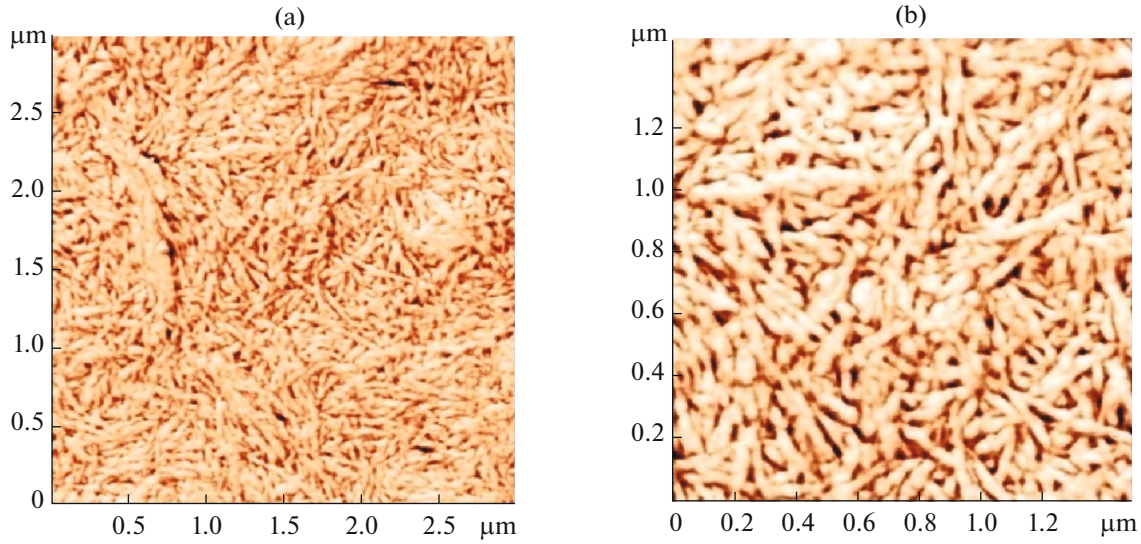

Fig. 2. Phase-contrast images of the NCC film surface obtained using the Solver 47 PRO AFM in the semicontact scanning mode at various magnifications.

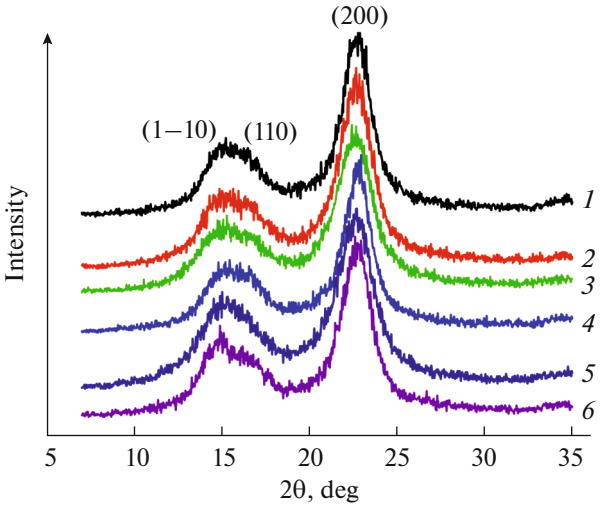

Fig. 3. Diffraction patterns of NCC films obtained (*1*) from an aqueous suspension of NCC; (*2*) when redispersing lyophilized NCC in acetonitrile; (*3*) when redispersing lyophilized NCC in methanol; (*4*) acetone gel in water; (*5*) acetonitrile gel in water; and (*6*) ethanol gel in water.

Morphology of lyophilized NCC. Drying by sublimation of NCC hydrosols makes it possible to obtain a material consisting of thin flakes that are formed on the surface of ice crystals (Figs. 4a–4c). The thickness of the flakes can be estimated from the SEM photograph (Fig. 4c) as 200–300 nm.

NCC organogels. All organogels in this work were obtained on the basis of dilute aqueous suspensions of NCC with a concentration of 1 g/L and pH 2.2. The photograph (Fig. 5) shows the appearance of an acetone organogel as an example. The photograph clearly shows that replacing water with the appropriate solvent (in this case, acetone) forms a dense gel that retains its shape well.

Redispersing of lyophilized NCC. The results of redispersing NCC dried from hydrosols with different pH are presented in Table 2.

Before discussing the results, it should be noted that the sizes of NCC particles obtained by the DLS method are averaged values for the hydrodynamic diameters of equivalent spheres and do not reflect the real physical dimensions of anisotropic rod-like particles of NCC, but are used for comparative analysis [43]. Nevertheless, as shown in [44], the hydrodynamic diameter measured by the DLS method strictly correlates with the length of the anisotropic NCC particle obtained from the analysis of TEM and AFM data. In addition, the analysis of the literature shows the emerging trend of the increasing use of DLS methods due to their simplicity and availability [45, 46].

From the data, it follows that the best redispersibility of lyophilized NCC is achieved in water and DMSO. The following regularity is observed: the higher the pH of the suspension from which the lyophilized samples were obtained, the smaller the size of the NCC particles upon redispersion of these samples in water and DMSO (Supplementary Materials, Figs. 1Sa, 1Sb). The charge of the NCC particles after repeated dispersing in water is retained and amounts to -38 ± 5 mV.

When the samples are redispersed in methanol, the size of the NCC particles does not depend on the pH of the suspension from which these samples were obtained and approaches the particle size in the initial aqueous NCC suspension (Supplementary Materials, Fig. 1Sf).

When redispersed in ethanol, in contrast to the initial NCC hydrosol, only one fraction of particles with a size of about 300 nm is observed (Supplementary Materials, Fig. 1Sg).

On redispersing in DMF, the size distribution of the NCC particles is, on the contrary, polydisperse. An increase in the pH of the hydrosol, from which the sample was prepared, causes (along with particles comparable in size to particles in the initial NCC suspension) the formation of aggregates 2.5–3 μm in size (Supplementary Materials, Fig. 1Sd).

In acetonitrile, the dispersion of both acidic NCC-2.2 and neutralized sample NCC-9.5 is accompanied by

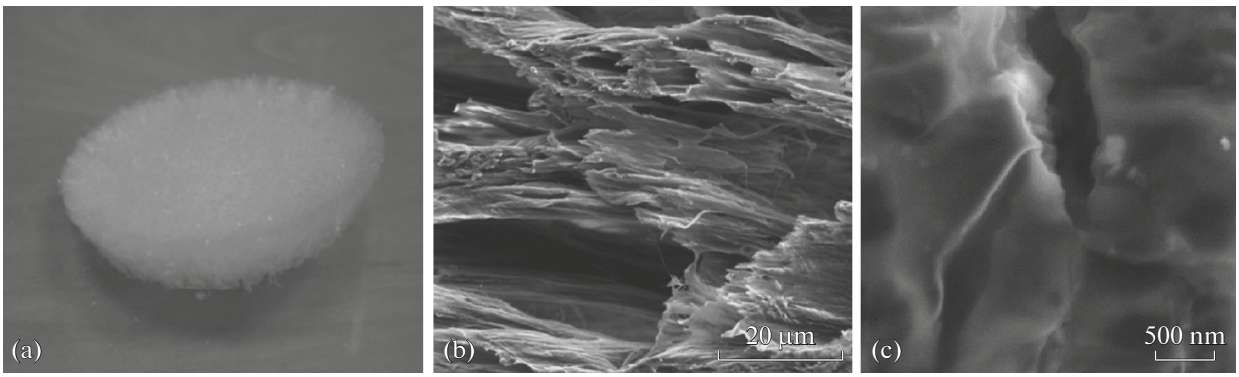

Fig. 4. External view of the NCC sample after freeze drying (a), images of the sample obtained using a scanning electron microscope with various magnifications (b, c).

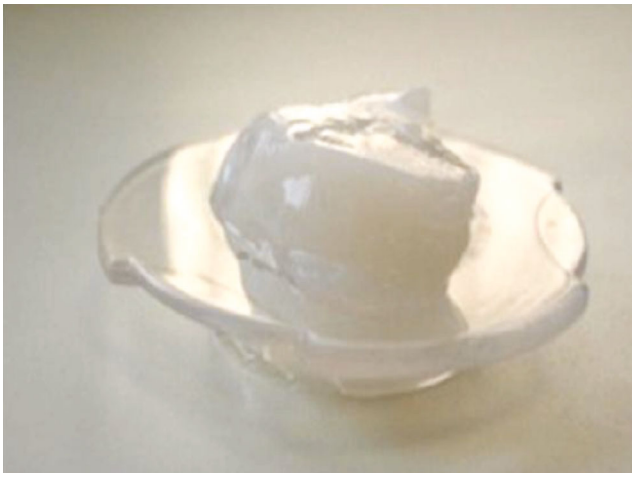

Fig. 5. Photo of an acetone organogel with an NCC content of 6%.

the formation of aggregates, which quickly precipitate and are not recorded by the device. Particles close in size to the initial NCC are formed upon dispersing of the NCC-4.0 sample in acetonitrile (Supplementary Materials, Fig. 1Se).

In all solvents, the dispersion of the NCC-2.2 sample leads to the formation of NCC particles, the sizes of which are larger than in the initial NCC hydrosol, and in DMSO and acetonitrile, aggregates with sizes above 3 μm are formed. An exception is the suspension of the NCC-2.2 sample in ethylene glycol, which is the most stable one for a long time (Supplementary Materials, Fig. 2S).

Analysis of the data shows that, in general, the ability of lyophilized NCC to disperse in organic solvents decreases with decreasing dielectric constant ε of the solvent. In solvents whose ε values are less than 24 (in our case, these are propanol, acetone, chloroform, and toluene), it was not possible to disperse the dried NCC. However, in dioxane, the dielectric constant of which is 2.2, samples NCC-2.2, NCC-4.0, and NCC-6.6 are redispersed. In this case, the particle size increases with an increase in the pH of the initial NCC hydrosol.

Redispersing of NCC organogels. The results of redispersing of acetone, acetonitrile, and ethanol NCC organogels are presented in Table 3 and in the Supplementary Materials (Fig. 3S).

Dispersion of acetone, acetonitrile, and ethanol organogels in most of the investigated solvents occurs with the formation of particles less than 100 nm. It is interesting to note that in two of the three solvents in which organogels are formed, acetone and acetonitrile, no dispersion occurs. There is no dispersion of

Table 2. Hydrodynamic diameter of particles upon redispersion of lyophilized NCC

Solvent	Solvent properties			Particle size, nm				
	ε	AN	DN kcal/mol	NCC-2.2	NCC-4.0	NCC-6.6	NCC-9.5	Dispersing degree
Water	78.5	54.8	18.0	90 ± 18 425 ± 22	30 ± 7 148 ± 28	5 ± 3 100 ± 15	19 ± 10 110 ± 12	Complete
DMSO	46.7	19.3	29.8	–	39 ± 12 148 ± 30	60 ± 5 230 ± 30	20 ± 10 110 ± 25	Complete
Ethylene glycol	37.7	–	(20)	294 ± 73 1186 ± 125	1294 ± 150	2025 ± 220	45 ± 6 846 ± 53	Complete
DMFA	36.7	16.0	26.6	389 ± 42	59 ± 12 230 ± 35	40 ± 8 166 ± 27 695 ± 95 2780 ± 260	25 ± 3 85 ± 5 355 ± 13 2780 ± 33	Partial
Acetonitrile	38.0	18.9	14.1	–	90 ± 3 285 ± 35	130 ± 25 415 ± 52	–	Partial
MeOH	32.6	41.3	19	–	50 ± 4 265 ± 24	230 ± 17	65 ± 10 295 ± 42	Partial
EtOH	24.3	37.1	19.2	555 ± 35	310 ± 55	265 ± 35	335 ± 47	Partial
i-PrOH	20.8	33.6	20.0	–	–	–	–	Not dispersed
Acetone	20.7	12.5	17.0	–	–	–	–	Not dispersed
Chloroform	4.7	23.0	0	–	–	–	–	Not dispersed
Dioxane	2.2	10.8	14.8	195 ± 25	555 ± 38	1280 ± 170	–	Partial
Toluene	2.4	–	0.1	–	–	–	–	Not dispersed

Table 3. Hydrodynamic diameter of particles upon repetitive dispersing of NCC organogels

Solvent	Solvent characteristics			Particle size, nm			
	ε	AN	DN, kcal/mol	acetone gel	acetonitrile gel	ethanol gel	dispersing degree
Water	78.5	54.8	18.0	60 ± 2	Complete	101 ± 3	Complete
DMSO	46.7	19.3	29.8	70 ± 5	Complete	75 ± 12 2060 ± 120	Complete
Ethylene glycol	37.7	–	(20)	45 ± 15	Complete	37 ± 2	Complete
DMFA	36.7	16.0	26.6	67 ± 17 15 ± 13	72 ± 13 15 ± 2	54 ± 5 2465 ± 115	Complete
Acetonitrile	38.0	18.9	14.1	–	–	–	Not dispersed
MeOH	32.6	41.3	19	90 ± 4	55 ± 4	72 ± 9	Partial
EtOH	24.3	37.1	19.2	240 ± 45	66 ± 10	89 ± 7	Partial
i-PrOH	20.8	33.6	20.0	595 ± 30 68 ± 32	55 ± 6	63 ± 3	Partial
Acetone	20.7	12.5	17.0	–	–	–	Not dispersed
Chloroform	4.7	23.0	0	–	–	–	Not dispersed
Dioxane	2.2	10.8	14.8	2790 ± 250	2615 ± 250	161 ± 23	Partial
Toluene	2.4	–	0.1	–	–	–	Not dispersed

organogels in chloroform and toluene. In dioxane, acetone and acetonitrile organogels are dispersed only with the formation of micrometer particles.

The surface charge of the NCC particles during the dispersion of organogels in water (similar to lyophilized NCC) is retained (the ζ-potential is -37 ± 4 mV).

CONCLUSIONS

The dispersion of lyophilized samples of nanocrystalline cellulose and NCC organogels (acetone, acetonitrile, and ethanol) in water and in organic solvents has been studied. It was shown that neutralization of the acidic form of NCC promotes an increase in redispersibility; however, for each solvent, there is an optimal pH value of the NCC hydrogel subjected to freeze-drying, which corresponds to the maximum dispersibility of lyophilized samples in a particular solvent. Dispersion of acetone, acetonitrile, and ethanol organogels in most of the studied solvents occurs with the formation of particles less than 100 nm.

ACKNOWLEDGMENTS

The data were obtained using the Verkhnevolzhskii Regional Center for Physicochemical Studies (center for collective use).

FUNDING

The work was supported by the Russian Science Foundation (project no. 17-13-01240).

COMPLIANCE WITH ETHICAL STANDARDS

The work does not involve experiments on animals or humans.

Conflict of Interests

Authors declare they have no conflicts of interests.

SUPPLEMENTARY MATERIALS

Supplementary materials can be found at https://doi.org/10.14258/jcprm.2019014240s.

REFERENCES

1. Peng, B.L., Dhar, N., Liu, H.L., and Tam, K.C., Chemistry and applications of nanocrystalline cellulose and its derivatives: A nanotechnology perspective, *Can. J. Chem. Eng.*, 2011, vol. 89, pp. 1191–1198. https://doi.org/10.1002/cjce.20554
2. Eichhorn, S.J., Cellulose nanowhiskers: Promising materials for advanced applications, *Soft Matter*, 2011,

no. 7, pp. 303–315.
https://doi.org/10.1039/c0sm00142b

3. Deepa, B., Abraham, E., Cordeiro, N., Mozetic, M., Mathew, A.P., Oksman, K., et al., Utilization of various lignocellulosic biomass for the production of nanocellulosea comparative study, *Cellulose*, 2015, vol. 22, pp. 1075–1085.
https://doi.org/10.1007/s10570-015-0554-x
4. Habibi, Y., Lucia, L.A., and Rojas, O.J., Cellulose nanocrystals: Chemistry, self-assembly, and applications, *Chem. Rev.*, 2010, vol. 110, pp. 3479–3500.
https://doi.org/10.1021/cr900339w
5. Eichhorn, S.J., Dufresne, A., Aranguren, M., Marcovich, N.E., Capadona, J.R., Rowan, S.J., Weder, C., Thielemans, W., Roman, M., Renneckar, S., Gindl, W., Veigel, S., Keckes, J., Yano, H., Abe, K., Nogi, M., Nakagaito, A.N., Mangalam, A., Simonsen, J., Benight, A.S., Bismarck, A., Berglund, L.A., and Peijs, T., Review: Current international research into cellulose nanofibres and nanocomposites, *J. Mater Sci.*, 2010, vol. 45, no. 1, pp. 1–33.
https://doi.org/10.1007/s10853-009-3874-0
6. Cao, X., Dong, H., and Li, C.M., New nanocomposite materials reinforced with flax cellulose nanocrystals in waterborne polyurethane, *Biomacromolecules*, 2007, no. 8, pp. 899–904.
https://doi.org/10.1021/bm0610368
7. Bondeson, D., Mathew, A., and Oksman, K., Optimization of the isolation of nanocrystals from microcrystalline cellulose by acid hydrolysis, *Cellulose*, 2006, vol. 13, no. 2, pp. 171–180.
https://doi.org/10.1007/s10570-006-9061-4
8. Araki, J., Wada, M., Kuga, S., and Okano, T., Flow properties of microcrystalline cellulose suspension prepared by acid treatment of native cellulose, *Colloids Surf. A.*, 1998, vol. 142, pp. 75–82.
https://doi.org/10.1016/S0927-7757(98)00404-X
9. Liu, D., Zhong, T., Chang, P.R., Li, K., and Wu, Q., Starch composites reinforced by bamboo cellulosic crystals, *Bioresour Technol.*, 2010, vol. 101, no. 7, pp. 2529–2536.
https://doi.org/10.1016/j.biortech.2009.11.058
10. Espinosa, S.C., Kuhnt, T., Foster, E.J., and Weder, C., Isolation of thermally stable cellulose nanocrystals by phosphoric acid hydrolysis, *Biomacromolecules,* 2013, vol. 14, no. 4, pp. 1223–1230.
https://doi.org/10.1021/bm400219u
11. Um, B.H., Karim, M.N., and Henk, L.L., Effect of sulfuric and phosphoric acid pretreatments on enzymatic hydrolysis of corn stover, *Appl. Biochem. Biotechnol.*, 2003, vols. 105–108, nos. 1–3, pp. 115–125.
https://doi.org/10.1385/ABAB:105:1-3:115
12. Yan, C.-F., Yu, H.-Y., and Yao, J.-M., One-step extraction and functionalization of cellulose nanospheres from lyocell fibers with cellulose II crystal structure, *Cellulose*, 2015, vol. 22, no. 6, pp. 3773–3788.
https://doi.org/10.1007/s10570-015-0761-5
13. Chen, L., Zhu, J.Y., Baez, C., Kitin, P., and Elder, T., Highly thermal-stable and functional cellulose nanocrystals and nanofibrils produced using fully recyclable organic acids, *Green Chem.*, 2016, vol. 18, pp. 3835–3843.
https://doi.org/10.1039/C6GC00687F
14. Espino-Perez, E., Domenek, S., Belgacem, N., Sillard, C., and Bras, J., Green process for chemical functionalization of nanocellulose with carboxylic acids, *Biomacromolecules*, 2014, vol. 15, no. 12, pp. 4551–4560.
https://doi.org/10.1021/bm5013458
15. Spinella, S., Maiorana, A., Qian, Q., Dawson, N.J., Hepworth, V., McCallum, S.A., Ganesh, M., Singer, K.D., and Gross, R.A., Concurrent cellulose hydrolysis and esterification to prepare a surface-modified cellulose nanocrystal decorated with carboxylic acid moieties, *ACS Sustain Chem. Eng.*, 2016, vol. 4, no. 3, pp. 1538–1550.
https://doi.org/10.1021/acssuschemeng.5b01489
16. Braun, B. and Dorgan, J.R., Single-step method for the isolation and surface functionalization of cellulosic nanowhiskers, *Biomacromolecules*, 2008, vol. 10, no. 2, pp. 334–341.
https://doi.org/10.1021/bm8011117
17. Cheng, M., Qin, Z., Chen, Y., Liu, J., and Ren, Z., Facile one-step extraction and oxidative carboxylation of cellulose nanocrystals through hydrothermal reaction by using mixed inorganic acids, *Cellulose*, 2017, vol. 24, pp. 3243–3254.
https://doi.org/10.1007/s10570-017-1339-1
18. Siqueira, G., Tapin-Lingua, S., Bras, J., da Silva Perez, D., and Dufresne, A., Morphological investigation of nanoparticles obtained from combined mechanical shearing, and enzymatic and acid hydrolysis of sisal fibers, *Cellulose*, 2010, vol. 17, no. 6, pp. 1147–1158.
https://doi.org/10.1007/s10570-010-9449-z
19. Filson, P.B., Dawson-Andoh, B., and Schwegler-Berry, D., *Green Chem.*, 2009, vol. 11, pp. 1808–1814.
https://doi.org/10.1039/b915746h
20. Torlopov, M.A., Udoratina, E.V., Maratov, I.S., and Sitnikov, P.A., Cellulose nanocrystals prepared in H3PW12O40–acetic acid system, *Cellulose*, 2017, vol. 24, no. 5, pp. 2153–2162.
https://doi.org/10.1007/s10570-017-1256-3
21. Torlopov, M.A., Mikhaylov, V.I., Udoratina, E.V., Aleshina, L.A., Prusskii, A.I., Tsvetkov, N.V., and Krivoshapkin, P.V., Cellulose nanocrystals with different length-to-diameter ratios extracted from various plants using novel system acetic acid/phosphotungstic acid/octanol-1, *Cellulose*, 2017, vol. 25, no. 2, pp. 1031–1046.
https://doi.org/10.1007/s10570-017-1624-z
22. Yahya, M., Lee, H.V., and Hamid, S.B.A., Preparation of nanocellulose via transition metal salt-catalyzed hydrolysis pathway, *BioResources*, 2015, vol. 10, no. 4, pp. 7627–7639.
https://doi.org/10.15376/biores.10.4.7627-7639
23. Chen, Y.W., Lee, H.V., and Hamid, S.B.A., Preparation and characterization of cellulose crystallites via Fe(III)-, Co(II)- and Ni(II)-assisted dilute sulfuric acid catalyzed hydrolysis process, *J. Nano Res.*, 2016, vol. 41, pp. 96–109.
https://doi.org/10.4028/www.scientific.net/JNanoR.41.96
24. Man, Z., Muhammad, N., Sarwono, A., Bustam, M.A., Kumar, M.V., and Rafiq, S., Preparation of cellulose nanocrystals using an ionic liquid, *J. Polym. Environ.*, 2011, vol. 19, no. 3, pp. 726–731.
https://doi.org/10.1007/s10924-011-0323-3

25. Miao, J., Yu, Y., Jiang, Z., and Zhang, L., One-pot preparation of hydrophobic cellulose nanocrystals in an ionic liquid, *Cellulose*, 2016, vol. 23, no. 2, pp. 1209–1219. https://doi.org/10.1007/s10570-016-0864-7

26. Zhang, J., [Wu, J., Yu, J., Zhang, X., He, J., and Zhang, J., Application of ionic liquids for dissolving cellulose and fabricating cellulose-based materials: State of the art and future trends, *Mater. Chem. Front.*, 2017, vol. 1, no. 7, pp. 1273–1290. https://doi.org/10.1039/C6QM00348F

27. Hirota, M., Furihata, K., Saito, T., Kawada, T., and Isogai, A., Glucose/glucuronic acid alternating copolysaccharides prepared from TEMPO-oxidized native celluloses by surface peeling, *Angew. Chem. Int. Ed.*, 2010, vol. 49, no. 42, pp. 7670–7672. https://doi.org/10.1002/anie.201003848

28. Hirota, M., Tamura, N., Saito, T., and Isogai, A., Water dispersion of cellulose II nanocrystals prepared by TEMPO-mediated oxidation of mercerized cellulose at pH 4.8, *Cellulose*, 2010, vol. 17, no. 2, pp. 279–288. https://doi.org/10.1007/s10570-009-9381-2

29. Montanari, S., Roumani, M., Heux, L., and Vignon, M.R., Topochemistry of carboxylated cellulose nanocrystals resulting from TEMPO-mediated oxidation, *Macromolecules*, 2005, vol. 38, no. 5, pp. 1665–1671. https://doi.org/10.1021/ma048396c

30. Peyre, J., Pääkkönen, T., Reza, M., and Kontturi, E., Simultaneous preparation of cellulose nanocrystals and micron-sized porous colloidal particles of cellulose by TEMPO-mediated oxidation, *Green Chem.*, 2015, vol. 17, pp. 808–811. https://doi.org/10.1039/C4GC02001D

31. Surov, O.V., Voronova, M.I., Rubleva, N.V., Kuzmicheva, L.A., Nikitin, D., Choukourov, A., Titov, V.A., and Zakharov, A.G., A novel effective approach of nanocrystalline cellulose production: Oxidation–hydrolysis strategy, *Cellulose*, 2018, vol. 25, no. 9, pp. 5035–5048. https://doi.org/10.1007/s10570-018-1910-4

32. Revol, J.-F., Bradford, H., Giasson, J., Marchessault, R.H., and Gray, D.G., Helicoidal self-ordering of cellulose microfibrils in aqueous suspension, *Int. J. Biol. Macromol.*, 1992, vol. 14, no. 3, pp. 170–172. https://doi.org/10.1016/S0141-8130(05)80008-X

33. Viet, D., Beck-Candanedo, S., and Gray, D.G., Dispersion of cellulose nanocrystals in polar organic solvents, *Cellulose*, 2007, no. 14, pp. 109–113. https://doi.org/10.1007/s10570-006-9093-9

34. Beck, S., Bouchard, J., and Berry, R., Dispersibility in water of dried nanocrystalline cellulose, *Biomacromolecules*, 2012, no. 13, pp. 1486–1494. https://doi.org/10.1021/bm300191k

35. Okura, H., Wada, M., and Serizawa, T., Dispersibility of HCl-treated cellulose nanocrystals with water-dispersible properties in organic solvents, *Chem. Lett.*, 2014, vol. 43, pp. 601–603. https://doi.org/10.1246/cl.131181

36. Siqueira, G., Fraschini, C., Bras, J., Dufresne, A., Prud'homme, R., and Laborie, M.-P., Impact of the nature and shape of cellulosic nanoparticles on the isothermal crystallization kinetics of poly(-caprolactone), *Eur. Polym. J.*, 2011, vol. 47, pp. 2216–2220. https://doi.org/10.1016/j.eurpolymj.2011.09.014

37. Bruckner, J.R., Kuhnhold, A., Honorato-Rios, C., Schilling, T., and Lagerwall, J.P.F., Self-assembly in cellulose nanocrystal suspensions using high-permittivity solvents, *Langmuir*, 2016, vol. 32, pp. 9854–9862. https://doi.org/10.1021/acs.langmuir.6b02647

38. Berg, O., Capadona, J.R., and Weder, C., Preparation of homogeneous dispersions of tunicate cellulose whiskers in organic solvents, *Biomacromolecules*, 2007, no. 8, pp. 1353–1357. https://doi.org/10.1021/bm061104q

39. Cheung, C.C.Y., Giese, M., Kelly, J.A, Hamad, W.Y., and MacLachlan, M.J., Iridescent chiral nematic cellulose nanocrystal/polymer composites assembled in organic solvents, *ACS Macro Lett.*, 2013, no. 2, pp. 1016–1020. https://doi.org/10.1021/mz400464d

40. Thygesen, A., Oddershede, J., Lilholt, H., Thomsen, A.B., and Stahl, K., On the determination of crystallinity and cellulose content in plant fibres, *Cellulose*, 2005, vol. 12, no. 6, pp. 563–576. https://doi.org/10.1007/s10570-005-9001-8

41. Elazzouzi-Hafraoui, S., Nishiyama, Y., Putaux, J.L., Heux, L., Dubreuil, F., and Rochas, C., The shape and size distribution of crystalline nanoparticles prepared by acid hydrolysis of native cellulose, *Biomacromolecules*, 2008, vol. 9, no. 1, pp. 57–65. https://doi.org/10.1021/bm700769p

42. French, A.D., Idealized powder diffraction patterns for cellulose polymorphs, *Cellulose*, 2014, vol. 21, no. 2, pp. 885–896. https://doi.org/10.1007/s10570-013-0030-4

43. Beck, S., Bouchard, J., and Berry, R., Dispersibility in water of dried nanocrystalline cellulose, *Biomacromolecules,* 2012, vol. 13, pp. 1486−1494. https://doi.org/10.1021/bm300191k

44. Boluk, Y. and Danumah, C., Analysis of cellulose nanocrystal rod lengths by dynamic light scattering and electron microscopy, *J. Nanopart Res.*, 2014, vol. 16, pp. 2174–2179. https://doi.org/10.1007/s11051-013-2174-4

45. Brinkmann, A., Chen, M., Couillard, M., Jakubek, Z.J., Leng, T., and Johnston, L.J., Correlating cellulose nanocrystal particle size and surface area, *Langmuir*, 2016, vol. 32, no. 24, pp. 6105−6114. https://doi.org/10.1021/acs.langmuir.6b01376

46. Beuguel, Q., Tavares, J.R., Carreau, P.J., and Heuzey, M.-C., Ultrasonication of spray- and freeze-dried cellulose nanocrystals in water, *J. Colloid Interface Sci.*, 2018, vol. 516, pp. 23–33. https://doi.org/10.1016/j.jcis.2018.01.035

Translated by N. Onishchenko